Dynamics of Salol at Elevated Pressure

R. Casalini,[†,‡] M. Paluch,[†,§] and C. M. Roland*[,†]

Naval Research Laboratory, Chemistry Division, Code 6120, Washington, D.C. 20375-5342, Chemistry Department, George Mason University, Fairfax, Virginia 22030, and Institute of Physics, Silesian University, Uniwersytecka 4, 40−007 Katowice, Poland

Received: August 9, 2002; In Final Form: January 23, 2003

The dielectric α relaxation was measured in salol over a range of temperatures at pressures as high as 0.7 GPa. The application of pressure causes a shift of the excess wing, relative to the primary α peak, indicating that the two processes have a distinct origin. Over all measured conditions, the response to pressure of the α relaxation and the dc-conductivity can be described as a volume-activated process, with the respective activation volumes exhibiting the same temperature dependence. When these results are compared to published viscosity data for salol, decoupling is observed at higher pressures and lower temperatures. The steepness index (T_g-normalized temperature dependence of the α-relaxation times) decreases with pressure by −0.011 per MPa. Near T_g, the relaxation is governed equally by volume and by thermal energy, the usual result for molecular glass formers in the absence of extensive intermolecular hydrogen bonding.

Introduction

The dynamics of supercooled liquids is a complex problem that continues to be the focus of many investigations. Among glass formers, salol has received significant attention, due to its simple molecular structure (Figure 1) and prototypical behavior. Light scattering,[1] dielectric spectroscopy,[2,3] specific-heat spectroscopy,[2] electron spin resonance,[4] and viscosity measurements[5] have all been brought to bear on the study of this intermediately fragile (steepness index ∼73)[6] liquid. Further insight into structural dynamics can be gained by extending the experimental parameters to include hydrostatic pressure. This is especially interesting in light of the dichotomy between associated liquids (e.g., hydrogen bonded) and those whose interactions involve predominantly van der Waals forces.[7] Generally, it is considered that pressure reduces the degree of hydrogen bonding,[8,9] although the effect may not be universal.[10] This means there are competing effects on the dynamics when pressure is applied. The presence of the hydroxyl and carbonyl moieties in salol suggests the possibility of hydrogen bond formation.

Light scattering spectra have been reported for salol under elevated pressure, both in the supercooled state[11] and above that regime.[12] The viscosity of salol has also been measured as a function of pressure.[13] This paper describes dielectric spectroscopy on salol obtained at pressures up to 0.7 GPa. The pressure dependence of the relaxation properties is determined and compared to results obtained by other experimental techniques. The relative contributions of volume and temperature to the relaxation times are also estimated.

Experimental Section

Salol (phenyl salicylate) was obtained from Aldrich and used as received. Dielectric measurements were carried out over 10 decades of frequency (10^{-4} to 10^6 Hz), using an IMASS time domain dielectric analyzer (10^{-4} to 10^4 Hz), and a Novocontrol Alpha analyzer (10^{-2} to 10^6 Hz). For high-pressure measurements, the capacitor (geometric capacitance ∼35 pF) was isolated from the pressurizing fluid with a Teflon ring. Pressure was applied using a manually operated pump (Enerpac), in combination with a pressure intensifier (Harwood Engineering). The sample was contained between parallel plate electrodes in a Manganin pressure cell (Harwood Engineering). The pressure was measured with a Sensotec tensometric transducer (resolution = 150 kPa).

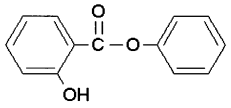

Figure 1. Phenyl salicylate (salol).

To circumvent crystallization, the sample was supercooled from the melt by rapid application of high pressure. At some lower pressure, crystallization would commence, as evident from a marked decrease of the dielectric strength and concomitant broadening of the relaxation peak. All data presented herein pertain to the wholly amorphous state.

Results and Discussion

Time−Pressure−Temperature Superpositioning. Representative dielectric loss spectra for salol at 36 °C and various pressures are shown in Figure 2. There is a systematic shift of the α-relaxation toward lower frequency with increasing pressure. At the highest pressures, the characteristic change in slope on the high frequency side of the peak (excess wing) can be seen. We have recently shown that the primary α-dispersion and the high-frequency excess wing for salol, when compared at the same value of the peak frequency (f_{max}), exhibit a different response to pressure.[14]

This is illustrated in Figure 3. The dielectric loss curves measured at ambient and elevated pressures superimpose in the vicinity of the peak maximum, but the spectra diverge at higher

* Author to whom correspondece should be addressed. E-mail: roland@nrl.navy.mil
† Naval Research Laboratory.
‡ George Mason University.
§ Silesian University.

10.1021/jp0267297 CCC: $25.00
Published on Web 03/07/2003

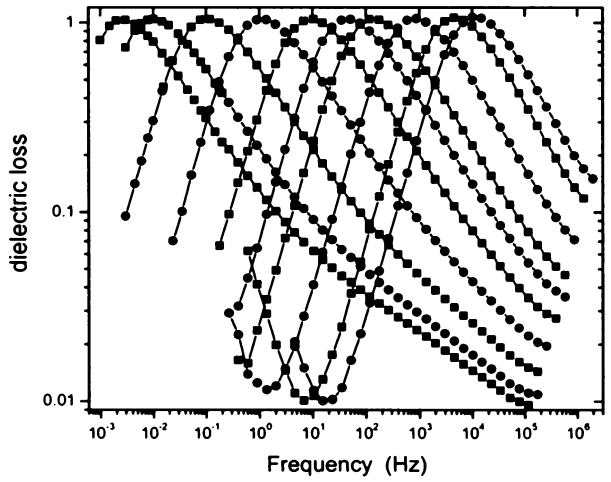

Figure 2. Representative dielectric loss curves for salol measured at 36 °C and pressures equal to (from right to left) 0.334, 0.352, 0.383, 0.414, 0.431, 0.460, 0.495, 0.528, 0.566, and 0.590 GPa.

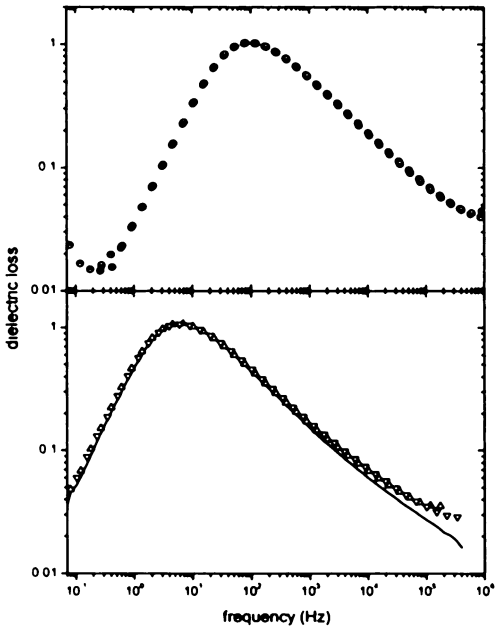

Figure 3. Lower pane: Structural relaxation peaks measured at −44 °C and ambient pressure[18] (—; frequency shift factor = 1.61; vertical shift factor = 0.71), at 24 °C and 0.383 GPa (△; no shifting), and at 50 °C and 0.567 GPa (▽; frequency shift = 0.87; vertical shift = 1.04). Upper Pane: Structural relaxation peaks at 36 °C and 0.414 GPa (◓; frequency shift = 0.7; vertical shift = 0.98) and at 46 °C and 0.492 GPa (◒; no shifting).

frequencies. This indicates that these two features reflect distinct processes; that is, the excess wing is not an inherent feature of the primary α-relaxation function. Such an effect is not observed in strictly van der Waals glass formers.[14] For all elevated pressures, however, the dielectric loss peak and the excess wing for salol superimpose at fixed τ_α ($= {}^1/_{2\pi f_{max}}$), as also shown in Figure 3.

When compared at a given value of τ_α, there is a modest broadening of the dispersion with increasing pressure (Figure 4). We believe that the behavior of the excess wing seen in Figure 3 (decoupling from the α-process under pressure) is related to the effect of pressure on the shape of α-peak. As discussed in detail elsewhere,[14−16] pressure changes the strength of intermolecular interactions (as reflected in the peak breadth), whereby the separation of the primary α-peak and the secondary (excess wing) relaxation increases. Also seen in Figure 4 is a

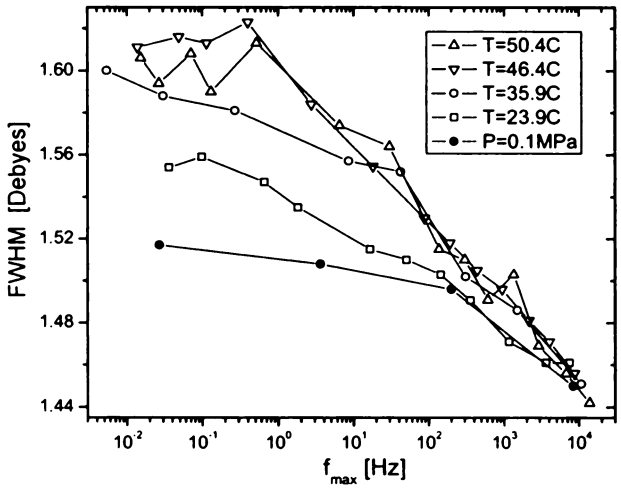

Figure 4. The breadth of the α peak for salol for various pressures (in the range 0.24 ≤ P (GPa) ≤ 0.7) at the indicated temperatures and at atmospheric pressure (data from ref 18).

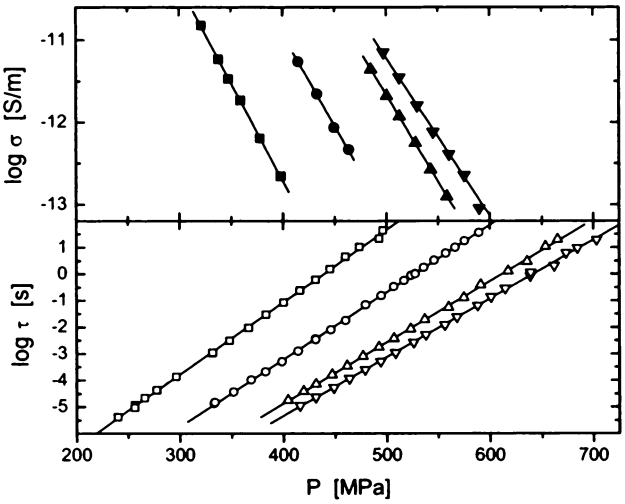

Figure 5. Pressure dependence of the relaxation times (hollow symbols) and dc-conductivity (solid symbols) for salol at T = 24C (□), 36 °C (○), 46 °C (△) and 50 °C (▽).

broadening of the spectra with increasing τ_α, attained by either higher pressure or lower temperature; similar behavior is observed in other glass formers.[17−20]

Activation Volume. The dielectric relaxation times are plotted in Figure 5 for all temperatures and pressures. Through the highest pressures measured herein, the relaxation times can be described as a simple volume-activated process

$$\tau_\alpha = \tau_0 \exp\left(\frac{P\Delta V_\tau}{RT}\right) \quad (1)$$

where ΔV_τ is a pressure-independent activation volume, τ_0 is a constant, and R is the gas constant. The activation volume is formally defined as

$$\Delta V \equiv \left.\frac{\partial G}{\partial P}\right|_T$$

where G is the Gibbs free energy. In combination with eq 1, this yields an Arrhenius form for the temperature dependence of τ_α, which is rarely observed. Thus, notwithstanding the linearity of the data in Figure 5, ΔV_τ herein is an apparent, rather than a true activation, volume. The ΔV_τ obtained from Figure 5 are displayed in Figure 6.

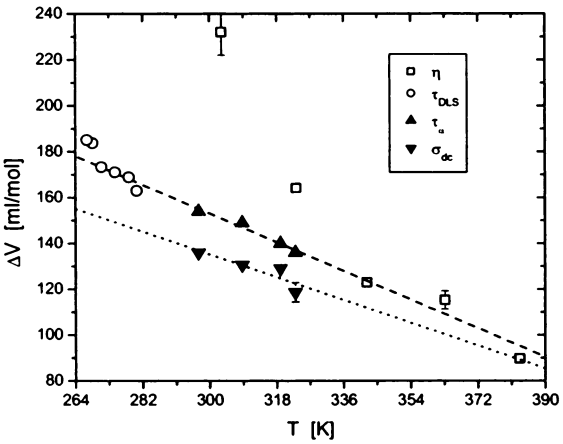

Figure 6. Activation volume determined from the pressure dependence of the dc-conductivity (▼), relaxation times (▲), viscosity[13] (□), and dynamic light scattering correlation times[11] (○). The dashed and dotted lines represent linear fits to τ_α and σ_{dc}, respectively.

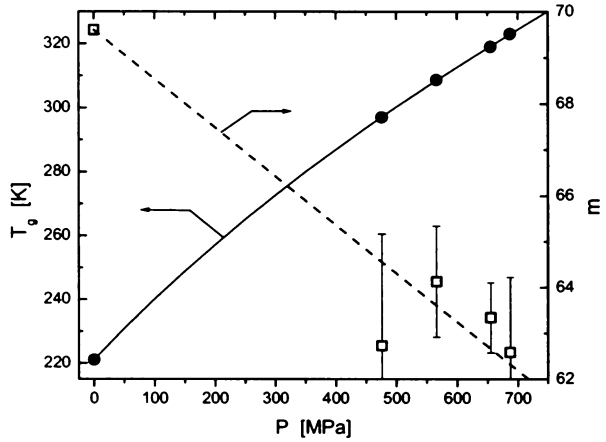

Figure 7. Left Axis: The temperature at which $\tau_\alpha = 10$ s (●), along with the fit to eq 3. Right axis: The steepness index (□) calculated from eq 4, with the dashed line representing a linear fit to data.

In the spectra at lower pressures in Figure 2, a contribution from the dc-conductivity, σ_{dc}, is seen at lower frequencies. This conductivity has a power law behavior in the dielectric loss

$$\sigma_{dc} = \epsilon_0 2\pi f \epsilon'' \tag{2}$$

where ϵ_0 is the permittivity of free space ($= 8.85 \times 10^{-12}$ F/m). Results for σ_{dc} at all four measurement temperatures are shown in Figure 5. The linear dependence on pressure yields values for the activation volume

$$\Delta V_\sigma = -RT \left.\frac{\partial \ln \sigma_{dc}}{\partial P}\right|_T$$

which are also displayed in Figure 6. The conductivity exhibits a weaker dependence on pressure than found for the relaxation times (i.e., smaller activation volume), although the temperature dependence of the respective ΔV are similar. Note that at atmospheric pressure, σ_{dc} and τ_α exhibit the same temperature dependence,[18] although structural relaxation in salol at constant pressure cannot be described as a thermally activated process.

Fragility. The glass transition temperature is commonly defined as the temperature at which the relaxation time assumes a value on the order of the experimental time scale, e.g., 10 s. The temperatures corresponding to this relaxation time are plotted as a function of pressure in Figure 7. The data conform to the empirical equation[21]

$$T_g(P) = T_g(0)\left(1 + \frac{b}{c}P\right)^{1/b} \tag{3}$$

with $T_g(P = 0) = -52.2$ °C, $b = 2.50$ and $c = 1.09$ GPa. The zero pressure limiting value of dT_g/dP is 204 ± 10% deg/GPa. This is intermediate among the values reported for small molecule glass formers.[22] (Note that the more commonly used reference value of $\tau_\alpha = 100$ s would require some extrapolation of the data in Figure 5, yielding a slightly smaller pressure dependence for T_g, with the glass temperature at atmospheric pressure being 3 deg lower.)

A useful measure of the temperature dependence of the dielectric relaxation times is from the fragility, defined as the steepness index

$$m = \left.\frac{d\log(\tau)}{d(T_g/T)}\right|_{T=Tg}$$

By use of the pressure coefficient of T_g (which itself is pressure dependent) and the activation volume, the steepness index can be calculated using the relation[23]

$$m = \frac{\Delta V_\tau}{\ln 10 R dT_g/dP} \tag{4}$$

The results are plotted in Figure 7, wherein m, equaling 70 at one atmosphere, is seen to be a decreasing function of pressure, $dm/dP \approx -0.011$ MPa^{-1}. Because the breadth of the peak increases slightly with pressure, salol represents an exception to the usual correlation of the fragility with the breadth of the relaxation function.[6]

The fact that pressure decreases the fragility may seem surprising, because the hydroxyl group in salol (Figure 1) should effect some hydrogen bonding, and pressure presumably reduces the degree of H-bonding.[8] Such breakup of the liquid structure embodies the concept underlying the term "fragile" (at least in its original conception[24]), thus implying that pressure should increase the dependence of τ_α on T_g-normalized temperature. However, the energy landscape interpretation of structural dynamics, from which this expectation is drawn, neglects explicit consideration of intermolecular constraints, and thus gives an incomplete accounting of the relaxation properties.[25−27]

Volume Dependence of τ_α. Knowledge of both the temperature and pressure dependences of τ_α allows an assessment of the relative contributions of thermal energy and volume to the structural relaxation properties. To do this, use is made of recent pressure−volume−temperature measurements on salol,[28] whereby the volume for any combination of temperature and pressure can be calculated. Accordingly, in Figure 8, the relaxation times from Figure 5 are displayed as a function of volume. Also included are the ambient pressure data of Stickel et al.[18] It is evident that changes in volume effected by temperature variations affect τ_α more strongly than do equivalent volume changes induced by pressure. This is, of course, because temperature alters the thermal energy as well as the volume.

This can be quantified by comparing the apparent activation energy for constant volume

$$E_V = R \left.\frac{\partial \ln \tau_\alpha}{\partial T^{-1}}\right|_V$$

to that for constant pressure

$$E_P = R \left. \frac{\partial \ln \tau_\alpha}{\partial T^{-1}} \right|_P$$ [29,30]

From interpolation of the data in Figure 8, τ_α for various fixed volumes is obtained. Isochoric τ_α for $V = 160$ and 164 mL/mol are shown in Figure 9. Extrapolation to the intersection with the atmospheric pressure data occurs at high temperatures (beyond the measured range of the atmospheric pressure data), with E_V/E_P approaching unity. This means that, at sufficiently high temperatures, whereupon the relaxation times exhibit an Arrhenius temperature dependence, thermal energy dominates the relaxation.

Of greater interest is the relative contribution of free volume for temperatures nearer T_g. However, assessment of this requires τ_α at higher volumes; that is, at pressures lower than the range of our measurements (which were limited by crystallization of the salol). To extrapolate the data in Figure 8, the Avramov equation[31,32] is used to describe the combined pressure and temperature dependencies. From this the relaxation times displayed in Figure 9 for $V = 169.6$ mL/mol were calculated. This particular volume is chosen because the isochoric data intersect the ambient pressure data at $\tau_\alpha = 1$s. The respective slopes in Figure 9 yield $E_V = 120$ and $E_P = 282$ kJ/mol. The uncertainty in E_V is quite large (ca., 50%), due to the extrapolation. Nevertheless, from the ratio, $E_V/E_P \approx 0.43 \pm 0.2$, we can conclude that neither temperature nor free volume is the dominant variable governing the relaxation times of salol near T_g.

The fact that temperature and volume make comparable contributions to the observed τ_α is consistent with results for a number of other glass formers.[7] On the other hand, substantially higher values of E_V/E_P (>0.9), reflecting a predominant effect of temperature, were determined for glycerol[33] and sorbitol.[34] These two associated liquids also exhibit weak pressure dependences;[23,34] their variation of T_g with pressure is more than a factor of 5 smaller than dT_g/dP obtained herein for salol. As we have previously pointed out,[7] the greater influence of thermal energy for liquids with extensive hydrogen bonding is likely due to the competing effects of compression; to wit, enhancement of steric constraints on local motion countervailed by a decrease in H-bond concentration.[8,9] We expect salol to be hydrogen bonded (viz., Figure 1). However, if it is intramolecular (to the carbonyl carbon), the pervasive intermolecular H-bonding of polyalcohols such as glycerol and sorbitol is absent, and thus temperature is not the dominant variable governing the relaxation of salol.

Comparison to Viscosity and Light Scattering Results. Upon approach to the glass transition, the temperature dependences of transport properties such as diffusion and the viscosity often differ from that of τ_α. This decoupling, arising from the heterogeneity inherent to the liquid state, can also be induced by pressure.[35] The viscosity, η, of salol was measured by Schug et al.[13] for various pressures. A comparison of these results with our τ_α data are displayed in Figure 10, for $T = 30$ °C (obtained by interpolating between τ_α measured at 20 and 36 °C), at 50 °C (τ_α directly measured), and 70 °C (by extrapolation from the τ_α at 65 °C). To compare η and τ_α, the respective ordinate scales were adjusted such that, for a given T, the two quantities coincide at ambient pressure. This is justified by the fact that at atmospheric pressure, η and τ_α are known to have the same temperature dependence.[18] As seen in Figure 10, at all temperatures, the viscosity data extend to lower pressures than the τ_α; the latter measurements are more limited by crystallization of the salol.

Decoupling of the viscosity and dielectric relaxation times is evident in Figure 10. However, the magnitude of the difference between their pressure dependences is reduced at higher temperatures, even though these data correspond to very high pressures (>0.5 GPa). The implication is that, at high temperature and low pressure, the viscosity and relaxation times are coupled. A similar conclusion was reached by Stickel et al.[18] from ambient pressure measurements on salol. However, for sufficient long values of the relaxation time (~msec or larger), as achieved at high pressures and lower temperatures, the two properties diverge. This result is consistent with the finding that the characteristic change in dynamics of supercooled liquids, as revealed by derivatives of Arrhenius plots of the relaxation times, transpires at a fixed value of τ_α, independent of temperature and pressure.[19,35]

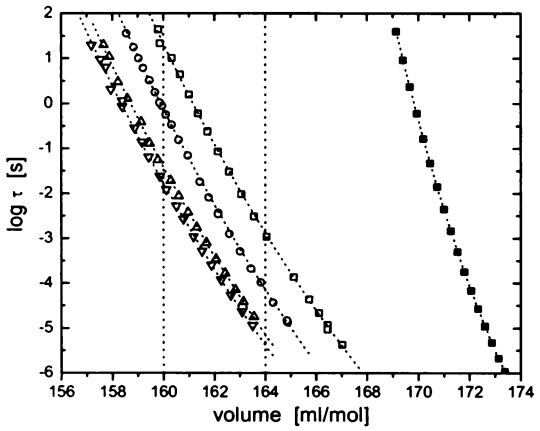

Figure 8. The relaxation times from Figure 5 plotted as a function of volume (24 °C, □; 36 °C, ○; 46 °C, △; 50 °C, ▽), along with atmospheric pressure data from ref 18 (●). The curves through the data points represent the linear fits to the data in Figure 5. The respective intersections of τ_α with the vertical dotted lines at $V = 160$ and 164 mL/mol are displayed in Figure 8 as a function of temperature.

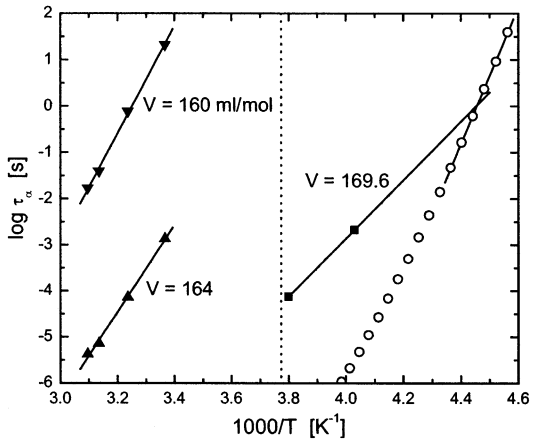

Figure 9. The isochoric relaxation times determined from the data in Figure 7 for the indicated volumes. The data for $V = 169.6$ (obtained by extrapolation of the measured relaxation times) intersect the atmospheric pressure data at $\tau_\alpha = 1$ s. The ratio of the respective slopes, $E_V/E_P = 0.43$, reflects the equal importance of temperature and volume.

From the data at the largest values of η, activation volumes

$$\Delta V_\eta = RT \left. \frac{\partial \ln \eta}{\partial P} \right|_T$$

are calculated and included in Figure 6. Reflecting the trends seen in Figure 10, as temperature is reduced (longer τ_α), ΔV_η becomes significantly larger than ΔV_τ (i.e., greater pressure sensitivity). Also shown in Figure 10 are activation volumes deduced from recent depolarized dynamic light scattering

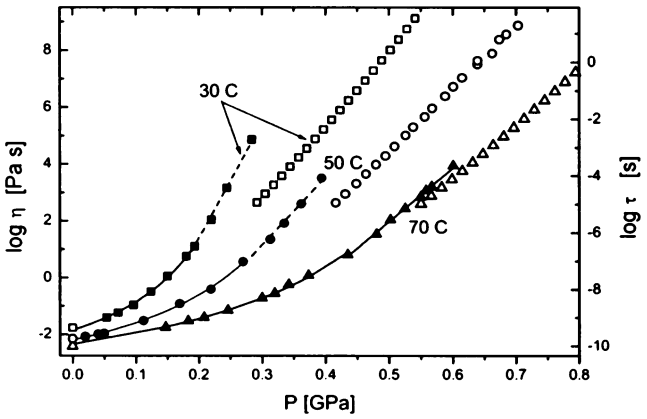

Figure 10. Viscosities[13] (solid symbols, left ordinate) and relaxation times (open symbols, right ordinate) for salol as a function of pressure. The τ_α at 50 °C are as measured, while the lower temperature τ_α are interpolations and the higher temperature τ_α are by extrapolation. The ordinate scales have been adjusted to make the atmospheric values of η and τ_α coincide. The lines through the viscosity points are only to guide the eyes.

measurements on salol at pressures up to 0.2 GPa.[11] The correlation times, τ_{DLS}, exhibit a pressure dependence quite similar to that of the relaxation times. This correspondence between the two is consistent with the molecular structure of salol (Figure 1). Reorientational modes that involve the dipole moment (arising from the electronegative oxygen atoms) will likewise cause fluctuations in the optical anisotropy (dominated primarily by the phenyl groups). This is quite different from the viscosity, reflecting center of mass displacements.

Summary

The following conclusions can be drawn from our analysis of the structural relaxation of salol under pressure:

1. The dielectric relaxation peak broadens with increasing τ_α, while there is a modest broadening of peaks measured at different T and P but having the same peak frequency. More interestingly, the α-peak and its high frequency excess wing respond differently to pressure, indicating that, although they may arise from related molecular motions, they are distinct processes, in agreement with other results.[36]

2. Activation volumes for the dielectric relaxation times, the dc-conductivity and the depolarized light scattering correlation times exhibit the same temperature dependence, while deviating markedly from the pressure dependence of the viscosity at higher pressures and lower temperatures.

3. In the limit of low pressure, $T(\tau_\alpha = 10s) = -52.2$ °C, with a pressure coefficient equal to 0.20 deg/MPa. The steepness index (fragility) decreases from a value of 70 at one atmosphere to ca. 63 at elevated pressure.

4. The ratio of the apparent activation energy at constant volume to that at constant pressure, calculated for $\tau_\alpha = 1$ s, is 0.43 ± 0.2. This implies that both thermal energy and volume exert a similar influence on the relaxation times. The value of this ratio is lower than previously found for strongly H-bonded polyalcohols,[33,34] and comparable to those of van der Waals liquids.[7] Such results are consistent with the idea that H-bonding in salol is, at least to some extent, intramolecular.

Acknowledgment. This work was supported by the Office of Naval Research. M.P. thanks the Committee for Scientific Research, Poland (KBN, Grant No. 5PO3B 022 20) for financial support. We thank J.J. Fontanella for experimental assistance, L. Comez for providing the data from references 11 and 28 prior to publication, H.E. King for helpful discussions and providing his viscosity results, K.J. McGrath for helpful discussions, and R. Richert for furnishing his dielectric data on salol at atmospheric pressure, which supplemented our own measurements therein.

References and Notes

(1) Sidebottom, D. L.; Sorenson, C. M. *Phys. Rev. B* **1989**, *40*, 461.
(2) Dixon, P. K. *Phys. Rev. E* **1990**, *42*, 8179.
(3) Wagner, H.; Richert, R. *J. Chem. Phys.* **1999**, *110*, 11660.
(4) Andreozzi, L.; Bagnoli, M.; Faetti, M.; Giordano, M. *J. Non-Cryst. Solids* **2002**, *303*, 262.
(5) Laughlin, W. T.; Uhlmann, D. R. *J. Phys. Chem.* **1972**, *76*, 2317.
(6) Bohmer, R.; Ngai, K. L.; Angell, C. A.; Plazek, D. J. *J. Chem. Phys.* **1993**, *99*, 4201.
(7) Paluch, M.; Casalini, R.; Roland, C. M. *Phys. Rev. B* **2002**, *66*, 092202. Paluch, M.; Casalini, R.; Roland, C. M.; Meier, G.; Patkowski A. *J. Chem. Phys.* **2003**, *118*, 4578.
(8) Naoki, M.; Katahira, S. *J. Phys. Chem.* **1991**, *95*, 431.
(9) Cook, R. E.; King, H. E.; Peiffer, D. G. *Phys. Rev. Lett.* **1992**, *69*, 30732.
(10) Root, L. J.; Berne, B. J. *J. Chem. Phys.* **1997**, *107*, 4350.
(11) Comez, L.; Fioretto, D.; Kriegs, H.; Steffen, W. *Phys. Rev. E* **2002**, *66*, 032501.
(12) Pratesi, G.; Bellosi, A.; Barocchi, F. *Eur. Phys. J. B* **2000**, *18*, 283.
(13) Schug, K. U.; King, H. E.; Bohmer, R. *J. Chem. Phys.* **1980**, *109*, 1472.
(14) Roland, C. M.; Casalini, R.; M. Paluch, M. *Chem. Phys. Lett.* **2003**, *367*, 259.
(15) Leon, C.; Ngai, K. L.; Roland, C. M. *J. Chem. Phys.* **1999**, *110*, 11585.
(16) Ngai, K. L.; Lunkenheimer, P.; Leon, C.; Schneider, U.; Brand, R.; Loidl, A. *J. Chem. Phys.* **2001**, *115*, 1405.
(17) Casalini, R.; Paluch, M.; Roland, C. M. *Phys. Rev. E* **2003**, *67*, in press.
(18) Stickel, F.; Fischer, E. W.; Richert, R. *J. Chem. Phys.* **1995**, *102* 6251; Stickel, F.; Fischer, E. W.; Richert, R. *J. Chem. Phys.* **1996**, *104*, 2043.
(19) Casalini, R.; Paluch, M.; Fontanella, J. J.; Roland, C. M. *J. Chem. Phys.* **2002**, *117*, 4901.
(20) Paluch, M.; Ngai, K. L.; Hensl-Bielowka, S. *J. Chem. Phys.* **2001**, *114*, 10827.
(21) Andersson, S. P.; Andersson, O. *Macromolecules* **1998**, *31*, 2999.
(22) Paluch, M.; Roland, C. M.; Best, A. *J. Chem. Phys.* **2002**, *117*, 1188.
(23) Paluch, M.; Casalini, R.; Hensel-Bielowka, S.; Roland, C. M. *J. Chem. Phys.* **2002**, *116*, 9839.
(24) Angell, C. A. In *Relaxations in Complex Systems*, Ngai, K. L., Wright, G. B., Eds.; National Technical Information Service, US Department of Commerce: Springfield, VA, 1985. Angell, C. A. *J. Non-Cryst. Solids* **1991**, *131−131*, 13.
(25) Roland, C. M.; Santangelo, P. G.; Ngai, K. L. *J. Chem. Phys.* **1999**, *111*, 5593.
(26) Santangelo, P. G.; Roland, C. M. *Phys. Rev. B* **1998**, *58*, 14121.
(27) Ngai, K. L.; Yamamuro, O. *J. Chem. Phys.* **1999**, *111*, 10403.
(28) Comez, L.; Fioretto, D.; Kriegs, H.; Steffen, W., to be published.
(29) Williams, G. *Trans. Faraday Soc.* **1969**, *60*, 1556; **1965**, *61*, 1564.
(30) Naoki, M.; Endou, H.; Matsumoto, K. *J. Phys. Chem.* **1987**, *91*, 4169.
(31) Avramov, I. *J. Non-Cryst. Solids* **2000**, *262*, 258
(32) Paluch, M.; Roland, C. M. *J. Non-Cryst. Solids* **2003**, *316*, 413.
(33) Ferrer, M. L.; Lawrence, C.; Demirjian, B. G.; Kivelson, D.; Alba-Simionesco, C.; Tarjus, G. *J. Chem. Phys.* **1998**, *109*, 8010.
(34) Hensel-Bielowka, S.; Paluch, M.; Roland, C. M. *J. Phys. Chem. B* **2002**, *106*, 12459.
(35) Casalini, R.; Paluch, M.; Roland, C. M. *J. Chem. Phys.* **2003**, *118*, in press.
(36) Casalini, R.; Roland, C. M. *Phys. Rev. B* **2002**, *66*, 18021.